Environ Geol (2009) 58:601–614
DOI 10.1007/s00254-008-1534-3

ORIGINAL ARTICLE

Environmental isotopic and hydrochemical study of groundwater in the Ejina Basin, northwest China

Y. H. Su · G. F. Zhu · Q. Feng · Z. Z. Li · F. P. Zhang

Received: 7 January 2008 / Accepted: 26 August 2008 / Published online: 10 September 2008

Abstract The study investigates the groundwater evolution and its residence time in the Ejina Basin, northwest China according to isotope and hydrochemical analyses results. The groundwater chemistry is mainly controlled by the dissolution of halite, Glauber's salt, gypsum, dolomite and calcite, also influenced by other processes such as evaporation, ion exchange, and deposition. Based on tritium content in atmospheric precipitation and by adopting a model with exponential time distribution function, the mean residence time of the unconfined aquifer groundwater with fairly high tritium activities (21–49 TU) is evaluated. The results show that these groundwaters have low residence time (5–120 years) and are renewable. In contrast, the deep confined groundwaters are tritium-free and radiocarbon values range from 18.3 to 26.7 pmc. According to the most commonly used ^{14}C correction models, the radiocarbon groundwater ages were calculated which yield ages of approximately 4,087–9,364 years BP. Isotopic signatures indicate formation of deep confined groundwaters in a colder and wetter climate during the late Pleistocene and Holocene. It is suggested that long-term, rational water usage guide should be set up for the Heihe River Basin as a whole to permit a considerable discharge to the Ejina Basin.

Keywords Ejina Basin · Environmental isotope · Hydrochemistry · Arid regions · Groundwater age

Y. H. Su (✉) · Q. Feng
Cold and Arid Regions Environmental and Engineering Research Institute, Chinese Academy of Sciences, 730000 Lanzhou, China
e-mail: syh@lzb.ac.cn

G. F. Zhu
The School of Mathematics, Physics and Software Engineering, Lanzhou Jiaotong University, 730000 Lanzhou, China

Z. Z. Li
Institute of Bioinformatics, School of Mathematics and Statistics, Lanzhou University, 730000 Lanzhou, China

F. P. Zhang
School of Mathematics and Information Sciences, Henan University, 475001 Kaifeng, China

Introduction

Arid zones in the northwest China including the whole Xingjing autonomous region, the Hexi Corridor in Gansu Province, and the area west of Helan Mountains in Inner Mongolia (Zhu et al. 2007) is one of the driest regions in the world (Shi and Zhang 1995). It is an eco-environmentally fragile area, which is characterized by low and irregular rainfall, high temperatures and evaporation, and notable drought periods (Ma et al. 2005). In such arid and semi-arid environments, groundwater is a significant part of the total water resource, and plays an important role as a water supply both for drinking and irrigation. Sustainable water management is vital for maintaining the ecosystem's balance and economic development (Narasimhan 2005; Esteller and Andreu 2004). The Ejina Basin has recently been the focus of attention due to increasing stress on its water resources and environmental degradation (Feng et al. 2004; Ji et al. 2005). The effective development and management of the valuable groundwater resources in the area require a better understanding of hydrochemical characteristics of the groundwater and its evolution under natural water circulation processes, as well as the origin and residence time of groundwater. During the last two

decades environmental isotope techniques have been commonly and largely used in the overall domain of water resources development and management (Fritz and Fontes 1980). The application of these relatively new techniques in the case of arid and semi-arid zones has proved to be an attractive tool for the identification of paleogroundwater and the quantitative evaluation of groundwater systems (IAEA 1980, 1983; Zuhair 2001).

In recent years, the Chinese government and scientists have carried out a number of studies on the assessment and utilization of water resources in Ejina Basin. Many works are focused on aspects such as utilization surveys, evolutionary prediction, reserve estimation and systematic assessment of natural water resources, and recognizing how to practice effective water management (Gao et al. 2004; Wu 1999). Comprehensive approaches to groundwater understanding using chemical and isotopic indicators are relatively few, although there are several investigations on the interaction and mechanism between surface water, groundwater and rock in recent years (Shi et al. 2001; Feng et al. 2004; Zhang et al. 2005; Zhu et al. 2007). Improved understanding of the fragile nature of the resource is fundamental to many decisions that will need to be made in China, in relation to demographic change and the reform of agricultural practices (Ma et al. 2005).

The purpose of this paper is, thus, to make a new assessment of the availability of groundwater resources in the Ejina Basin as the typical area of arid northwest China (Fig. 1a) on the basis of a better understanding of hydrogeological features. The specific targets are to (1) identify sources of recharge, to localize recharge areas; (2) determine the predominant geochemical process taking place along the inferred horizontal groundwater flow line and (3) determine the groundwater residence time by employing isotopic measurements. These may provide a theoretical basis to the government for developing suitable water resource utilization strategies and policies for northwestern China in this new century.

The study area

The Ejina Basin (40°20′ and 42°30′ N, 99°30′ and 102′00′ E) is in the lower reaches of the Heihe River, starting from Dingxin town in Gansu province down to the boundary between China and Mongolia, confined by the Baddain Jaran Desert in the east and by the Beishan Mountains in the west (Fig. 1a). Generally, the ground of the basin slopes from southwest to northeast by degrees, having the feature of low in the middle and high all around. The basin elevations range from 898 to 1,598 m above sea level (Wen et al. 2005). The climate of the study area is highly continental, with a long dry season from October to June, and a 3-month rainy season from July to September, which contributes 60–70% of the total rainfall. The mean annual precipitation is only 42 mm, whereas the potential evaporation is as high as 3,755 mm. A winter minimum temperature of −38.5°C and a summer maximum of 43.1°C have been recorded, and the day–night temperature difference can reach 28–30°C. Because of sparse and highly variable precipitation, no perennial runoff originates from the area. The Heihe River originating from the Qilian mountains of Qinghai provinces with a length of 821 km is the only runoff flow from this area. At Langxinshan Mountain, the Heihe River separates into two branches: the east river and the west river, both flowing north and reaching East and West Juyan Lake, respectively (Fig. 1a).

The total runoff of Heihe River coming from Qilian Mountain outlets is about 37.55×10^9 m^3 (Gao and Li 1990). Surface runoff from the upper mountain area by rain, melt water of snow and glaciers is the only source of water available in the whole Heihe River Basin. The intensive exploitation of the water resources in the middle oases area, mainly for irrigation of agricultural land, has resulted in the decrease of surface water supply for the Ejina Basin. In the 1950s, the annual discharge of the Heihe River into the Ejina Basin was about 12×10^9 m^3; however, in the 1990s, it was less than 7×10^9 m^3 (Xiao 2000; Gao et al. 2004). The eastern and western branches of the Heihe River in its lower reaches have become intermittent rivers since the 1960s. The West Juyan Lake and the East Juyan Lake have dried up since 1961 and 1992, respectively (Chen 1996).

Geological and hydrogeological frameworks

In terms of the geotectonic characteristics, from its source at the northern margin of the Qinghai-Tibet Plateau the Heihe River transects three different geological units: (1) the southern Qilian Paleozoic geosynclinal fold zone, (2) the middle Hexi Corridor depression (Zhangye Basin) with its associated structures, and (3) the northern Ejina Basin, limited to the north by Alasha fault-block uplift structural zone (Fig. 1a). The subduction of the Indian Plate under the Eurasian Plate caused the Qinghai-Tibet Plateau to become uplifted and pushed to the north (Molner and Tapponnier 1975; Harrison et al. 1992). The uplift of the Qilian geosyncline occurred from the end of the Palaeozoic and continuing through the whole Mesozoic era, and created the embryonic form of the Hexi Corridor. This was followed by a complex tectonic episode when the Longshou–Heli Mountain structural zone was formed in the middle of the Hexi Corridor; dissecting the whole Corridor into two parts: the southern and the northern sub-basin. From the late Tertiary, especially from the end of the Pliocene and the beginning of the early Pleistocene, the

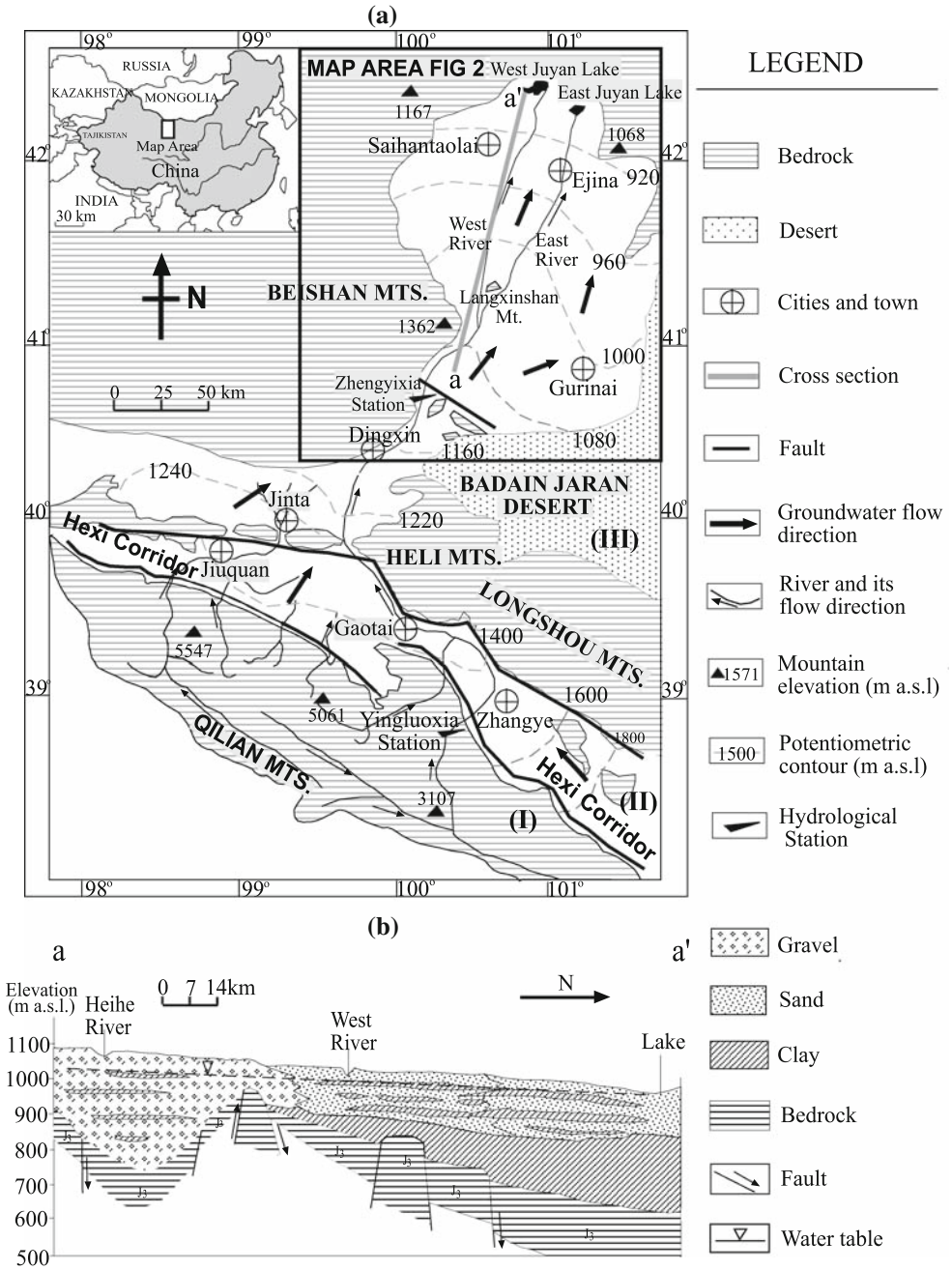

Fig. 1 **a** The setting of the Heihe River Basin showing the hydrological systems in relation to the main flow direction of groundwater and surface water towards the terminal lakes. The geological cross-sections of **b** (a–a′) are indicated. The main hydrogeological regions linked to the geological structure are shown (I–III). **b** Hydrogeologic cross-sections along transect a–a′ in a

surrounding Tibetan mountains underwent a rapid uplift (Li et al. 1979) and the basin subsided further. Resulting from this period of activity, a series of NW–SE faults were formed along the piedmont (Fig. 1a). At the same time the intensive denudation and erosion from the mountains led to significant transfer of clastic material to the basin. This formation of thick Quaternary diluvial and alluvial sediments, and some eolian and lacustrine deposits, led to the formation of the main aquifer.

In the southern part of the southern sub-basin, the piedmont alluvial aquifer is formed of highly permeable cobble and gravel deposits with a thickness of some 300–500 m. The aquifer system belongs to one-layer unconfined aquifer which the present day water levels range between 50 and 100 m below surface. The coefficient of permeability is about 5–120 m/day in the piedmont aquifer with a hydraulic gradient ranging from 3 to 8‰. The transmissivity ranges from 2,000 to 10,000 m^2/day (Fan 1991). This allows a large

amount of surface runoff in the piedmont fan to seep down and recharge the aquifer. In natural conditions, more than 80% of the surface water formed by melting ice–snow, precipitation and the springs in the Qilian Mountains entering the basins infiltrates into the alluvial piedmont aquifer and transforms to groundwater, about 26.6×10^8 m^3 (Wu et al. 2004). From the northern edge of the alluvial fans, the aquifer comprising inter-bedded gravel, coarse sand, fine sand and clay becomes several layers of confined or semi-confined aquifer with the burial depth of the aquifer less than 5 m depth. In many places at the onset of confined conditions, the groundwater then overflows as springs and re-emerges as stream. There are two main groundwater flow directions based on the water table contours map: from SE towards NW and from the SW towards the NE (Fig. 1a). The existence of tectonic uplifted zone in the middle of the Hexi Corridor such as Heli–Longshou Mountain and some small hills led to groundwater barely crosses the fracture from south sub-basin to recharge the north sub-basin.

Bedrock in the northern sub-basin consists of Sinian schist, gneiss, limestone, metamorphic sandstone, Palaeozoic sandstone, and inter-bedded Jurassic and Tertiary sandstone and shale. The schists contain mostly quartz and are micaceous. Besides these, there are shales and sandstones containing limestone. The Pliocene and early Pleistocene sediments in the northern sub-basin are interbed, poorly consolidated fluvio-lacustrine sandstones (Fan 1991). The overlying Middle and Late Pleistocene sediments are composed of fluvial gravel in the south of the basin but inter-bedded sand and clay extend northward (Fig. 1b). The Quaternary sediments are rich in evaporite minerals such as halite, gypsum and Glauber's salt (Zhu et al. 2007). The depth to the water table is 10–30 m in the southern part of this sub-basin and gradually changes to 3 m below the surface in the Ejina City (Fan 1991). The aquifer system transformed from a one-layer unconfined aquifer to a multi-layer unconfined–confined aquifer system. The one-layer unconfined aquifer is mainly distributed in the south of this northern sub-basin with a thickness ranging from 150 to 200 m or more. It is composed of alluvial–pluvial coarse sand and gravel intercalated with lenticular bodies of clay and silt (Fig. 1b). The multi-layer aquifer system can be found in the northern part of the sub-basin with a total thickness of about 150–180 m, and in some regions can reach 300 m. The confined aquifer is deeper than 70 m, and consists of gravelly sand, loam sand, occasionally with discontinuous impermeable thin layers of clay, and silty clay. About 68% of the seasonal river water recharges groundwater (Wen et al. 2005). The hydraulic conductivity of the shallow aquifer ranges from 11.0 to 12.3 m/day with a gradient ranging from 1 to 1.7‰; From south to north (within the northern part of the northern sub-basin), the conductivity of the confined aquifer decreases from 3.87 to 0.56 m/day, and the gradient decrease from 1.6 to 1‰ (Fan 1991). Analytical results of groundwater chemistry and groundwater level data from the center of the northern sub-basin show that the deep groundwater flow system recharges the shallow groundwater flow systems (Zhu et al. 2004). Shallow groundwater is lost to vertical surface evaporation and desert vegetation transpiration. The groundwater in the northern sub-basin flows from the southwest to the northeast (Fig. 1a).

Materials and methods

Samples were taken for chemical and isotopic analysis during May and October 2002. A total of 19 groundwater samples were obtained from the water-supplying wells are within the Quaternary aquifer and these fell into two distinct groups (shallow wells with depths <15 m, and deep wells with depths ranging from 50 to 150 m) corresponding to the customary drilling practice; surface water samples were taken from the Heihe River as well as the West/East Juyan Lakes. The location of sampling sites is shown in Fig. 2.

Total alkalinity (as HCO_3^-), electrical conductivity (EC), pH, temperature, and redox potential (eH) were measured in the field using an in-line flow cell to ensure the exclusion of atmospheric contamination and to improve measurement stability. Alkalinity was measured using a Hath® field titration kit. The EC, pH, temperature and Eh

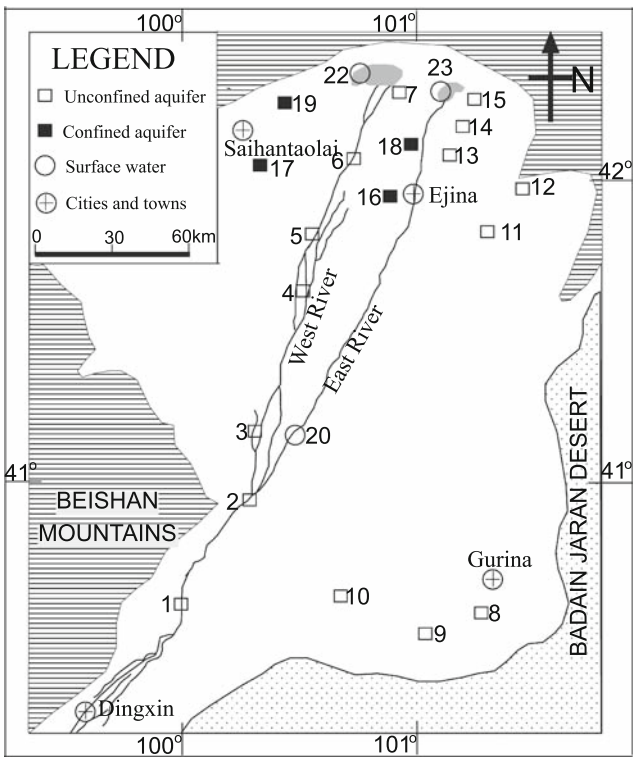

Fig. 2 Site map of the Ejina Basin showing the sampling locations

was measured using portable Orion EC and pH meters. Groundwater was collected after pumping the wells for 15–20 min. Samples were subsequently filtered at 0.45 μm and collected in acid-washed, well-rinsed low density polyethylene bottles. Filtered and acidified (1% v/v HNO_3) samples were analyzed for major cations, SO_4^{2-}, and a wide range of trace elements either by inductively coupled plasma optical emission spectrometer (ICP-OES) or inductively coupled plasma mass spectrometry (ICP-MS); while filtered and unacidified samples were analyzed for chloride, NO_3–N, Br, F and I by automated colorimetry. Chemical analyses were measured at the Geochemistry Laboratory of the Cold and Arid Region Environmental and Engineering Institute, Chinese Academy of Sciences, Lanzhou P. R. China. Calibrations for cation analyses were performed using appropriately diluted standards, and both laboratory and international reference materials were used as checks for accuracy. Instrumental drift during ICP-MS analysis was corrected using In and Pt internal standards. The analytical precision for measurement of ions was determined by calculating the ionic balance error, which is within 5%.

Samples for $\delta^{18}O$, δD and tritium were collected in 1 l glass bottles with gas-tight caps. The samples were prepared for dissolved inorganic carbon and subsequent carbon isotope determination, by adding excess $BaCl_2$ to 120 l of water previously brought to pH $\geq$12 by addition of CO_2-free NaOH and collecting the precipitated $BaCO_3$. The $\delta^{18}O$, δ^2H, $\delta^{13}C$, tritium, and ^{14}C analyses were performed in Isotope Laboratory of Lanzhou Institute of Seismology of China. Samples for stable isotope analysis (^{18}O, ^{2}H, ^{13}C) were measured by isotope ratio mass spectrometry (VG Micromass 602C). Stable isotopic data are expressed in the conventional δ-permille (δ ‰) notation referenced to Vienna Standard Mean Ocean Water (V-SMOW) for ^{18}O and ^{2}H, and Vienna Pee Dee Belemnite (V-PDB) for ^{13}C. The analytical reproducibility is ±0.1‰ for $\delta^{18}O$, and ±1% for δ^2H, $\delta^{13}C$. Samples for tritium were electrolytically enriched and analyzed with a Quantulus-1220 Liquid Scintillation Beta Spectrometer. The results were reported as tritium units with a typical error of ±0.1–0.2 TU (Eichinger 1980). The ^{14}C of dissolved inorganic carbon (DIC) was determined radiometrically by liquid scintillation counting after conversion to benzene. The results of radiocarbon are reported as percent modern carbon (pmc) with an analytical uncertainty of ±0.3 pmc.

Results

Chemical composition of groundwater

The hydrochemical properties of groundwater samples collected from the Quaternary aquifer system are shown in Table 1. The sites from which samples were taken are shown in Fig. 2.

The pH value in groundwater ranges from 7.18 to 8.90 with an average value of 7.72, indicating an alkaline nature. The total dissolved solids (TDS) of groundwater ranges from 674 to 6,576.8 mg/l with an average of 2,304.7 mg/l and a standard deviation of 2,012.5 mg/l. The plot of chemical analyses on a trilinear diagram (Fig. 3) of groundwater along with surface water shows that a majority of groundwater samples fall in the 'no-dominant' class, and a number of samples are of sulphate type in the anion facies, while some shallow groundwater samples from the terminal lakes are of chloride type. Among the cation facies, the majority of the water samples are of sodium or potassium type, and the rest fall in the class of 'no-dominant' type. None of the samples are of calcium type. Finally, the groundwater types in the study area are identified spatially and indicate an obvious zonation as shown in Fig. 4: (1) the $Na^+ \cdot HCO_3^-$ type occurred near the bank of the Heihe River and in the Gurina Swamp Zone. Replenishment for most of these groundwaters came from the rapid seepage flow of river water. The concentration of TDS in the groundwater is mostly less than 1,000 mg/l, belonging to fresh water. The HCO_3^- and SO_4^{2-} are the major anions and Na^+ is the major cations in the groundwater; (2) In the intermediate zone of groundwater recharge and discharge areas, water type transformed into $Na^+ \cdot Mg^{2+} \cdot SO_4^{2-} \cdot Cl^-$ or $Na^+ \cdot Mg^{2+} \cdot Cl^- \cdot SO_4^{2-}$. This type of water represented high TDS water ranging from 1,000 to 3,800 mg/l (sample nos. 13–15). The groundwater belonged to the slightly saline or the moderately saline water. The major anions in the groundwater were SO_4^{2-} and Cl^- and the major cations were Na^+ and Mg^{2+}; (3) The $Na^+ \cdot Cl^-$ type of water was dominant in the Jisuituhaizi area. The groundwater had strong evapotranspiration, and this groundwater type represented the high TDS, more than 5,000 mg/l (sample nos. 11 and 12), belonging to the very saline or briny water. The major anion in the groundwater was Cl^- and the major cation was Na^+.

Isotopic composition of groundwater

The results of stable isotope analysis both for water samples in the basin and precipitation collected in Zhangye meteorological station since 1986 (from the IAEA database) are plotted in Fig. 5. Values of $\delta^{18}O$ and δ^2H in precipitation vary over a large range from −24.74 to 0.87‰ and −191.4 to −4.3‰, respectively, but they are linearly similar to global meteoric water line (GMWL) with an equation of $\delta^2H = 6.87\delta^{18}O - 3.49 (r^2 = 0.94)$, which is defined as local meteoric water line (LMWL). These values are slightly enriched and indicate modification due to

Table 1 Chemical and isotope composition of water samples in the study area

Site no.	pH	HCO_3^- (mg/l)	Cl^- (mg/l)	SO_4^{2-} (mg/l)	Ca^{2+} (mg/l)	Mg^{2+} (mg/l)	K^+ (mg/l)	Na^+ (mg/l)	TDS (mg/l)	$\delta^{18}O$ (‰)	δ^2H (‰)	Tritium (TU)	$\delta^{13}C$ (‰)	^{14}C (pmc)
Unconfined														
1	8.00	236.2	57.9	225.3	58.7	49.7	4.3	84.4	716.5	−6.9	−46	37		
2	7.85	231.9	68.5	208.5	47.1	50.7	5.9	82.6	695.2	−7.6	−42	32		
3	7.92	280.1	150.2	316.5	43.1	37.2	9	224	1,060.1	−7.6	−51	42		
4	7.52	286.2	73.5	235.4	57.9	49.3	18.3	100.1	820.7	−7.5	−52	32		
5	8.01	184.3	127.1	308.8	40.5	51.2	9	147	867.9	−7.1	−47	–		
6	7.90	230.1	104.7	187.8	33.1	37.7	9	129	731.4	−7.7	−48	–		
7	7.93	217.8	113.3	440.4	72.8	54.2	6.6	163.1	1,068.2	−6.9	−45.8	49		
8	7.34	272.8	117.9	160.9	31.5	15	11.7	192.1	801.9	−3.5	−56	29	−6.3	65
9	7.29	228.2	132.8	142.2	18.6	20.6	16.4	186.1	744.9	−3.4	−48	30		
10	7.18	228.2	72.1	101.8	13.6	11.3	13.3	150	590.3	−2.3	−46	23		
11	7.25	344.2	1,325.2	259.6	407.2	211.5	58.1	1,155.1	5,960.9	−8.1	−56.7	–		
12	7.40	920.2	2,923.1	909.9	207	579.6	28.9	1,008.1	6,576.8	−8.0	−55.5	21		
13	7.88	580.3	547.1	161.0	220.2	282.2	30	580.1	3,800.9	−6.0	−52	–		
14	7.90	422.9	178.2	170.5	117.6	18.1	9.8	176	1,093.1	−5.9	−47	–		
15	7.58	124.5	548.5	565.3	96	16.1	2	525.5	1,877.9	−7.3	−47.8	38		
Confined														
16	8.90	251	45.9	130	50	32.9	5.7	52	567.5	−9.6	−66.2	<1	−4.6	26.4
17	7.70	320.9	347.2	934.5	123.8	96.7	3.7	446	2,272.8	−9.7	−68	<1	−5.9	22.4
18	7.50	97.6	420.5	567.5	22.8	109.8	2.8	352.8	1,574.9	−10.3	−70.2	<1	−5.9	26.7
19	7.60	203.8	63.9	211.9	52.9	47.9	3.9	93.6	674	−11.1	−78.8	<1	−6.5	18.3
Surface water														
20	7.19	207.5	50.1	106.4	40.2	36.8	4.2	48.1	493.3	−7.1	−44.5	42		
21	7.22	228.2	55.4	126.3	49.9	43.8	4.7	54.6	562.9	−6.9	−41.9	29		
22	8.15	244.2	120.2	207.7	52.2	66.4	9.2	149.9	849.8	−5.0	−53	–		
23	7.91	424.1	104.5	280.4	49.1.8	57.7	8.1	180.4	1,055.2	−6.6	−55.4	–·		

evaporation in the monsoon rains producing departure from the GMWL. Weighted mean rainfall values at Zhangye station for seven non-consecutive years since 1986 lie around $\delta^{18}O$ −6.51‰ and δ^2H −44‰. These values are most likely to be representative of present day local waters.

For the stable isotope composition of the Heihe River running course, the mean values of $\delta^{18}O$ increase along the river course. The $\delta^{18}O$ and δ^2H values for these samples ranged from −7.1 to −6.9 and −44.5 to −41.9‰, respectively (Table 1) and with the mean $\delta^{18}O$ values of −7.0‰. Figure 5 illustrated that the samples from the Heihe River running course have the similar stable isotope compositions to those from the wells drilled into the unconfined aquifers near the river bank. In contrast, the surface water collected from the West/East Juyan Lakes have slightly heavier isotopic compositions of −6.6 to −5.0‰ $\delta^{18}O$ and −55.4 to −53‰ δ^2H (Table 1)and with a mean $\delta^{18}O$ values of −5.8‰. The surface water evaporation line, $\delta^2H = 0.875\delta^{18}O - 48.635 (r^2 = 0.93)$, was obtained by the least squares fit (LSF) method using the open water bodies in the Weat/East Juanyan Lakes, and produces an intercept near to the mean modern rainfall values for Zhangye. The 'deuterium excess' values d ($d = \delta^2H - 8\delta^{18}O$, Dansgarrd 1964) for the surface water samples ranged from −29.2 to 3.2‰ with a mean value of −14.1‰. These values are significantly lower than 10‰, the value estimated by Craig (1961) for the global meteoric waters. This indicated that evaporation is probably occurring in ponds, reservoirs and swamps in the study area.

The unconfined aquifer groundwater has $\delta^{18}O$ values in the range of −8.1 to −2.3‰ and δ^2H from −56.7 to −42‰ (Table 1). The average values of $\delta^{18}O$ and δ^2H in the unconfined aquifer are −6.35 and −49.6‰, respectively. The deep confined groundwater has $\delta^{18}O$ values in the range of −11.1 to −9.6‰ and δ^2H from −71.8 to −61.2‰ (Table 1). The average values of $\delta^{18}O$ and δ^2H in the unconfined aquifer are −10.2 and −65.3‰, respectively. Several observations may be made about the stable isotopes in the groundwater in relation to the surface water as well as modern rainfall. First, the majority of the isotope compositions of the groundwater samples plot close to the

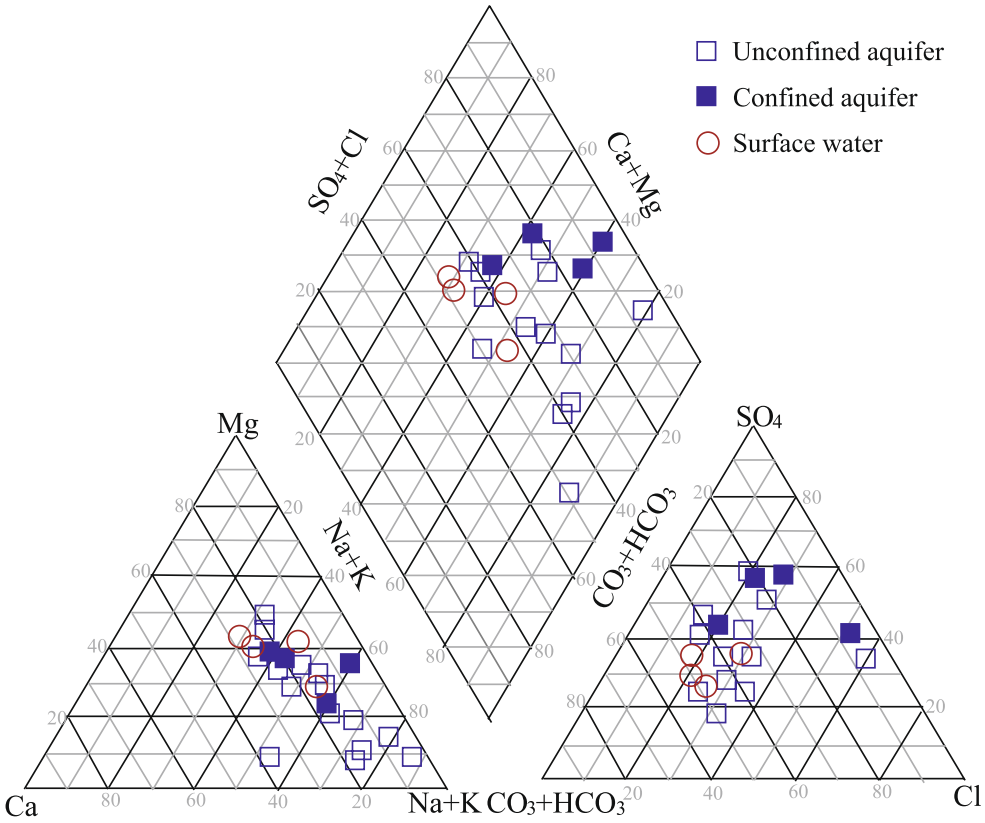

Fig. 3 Piper plot of chemical analysis of groundwater and surface water samples in the Ejina Basin

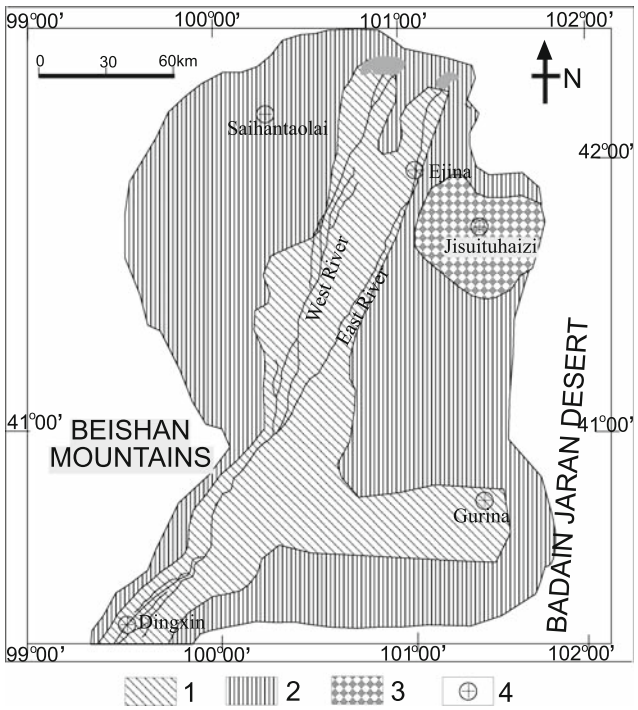

Fig. 4 Spatial distribution of groundwater quality types with sampling sites in the study area. *1* TDS is less than 1,000 mg L^{-1} and the water type is $Na^{+}{\cdot}HCO_3^{-}$; *2* TDS is between 1,000 and 3,500 mg L^{-1} and the water type is $Na^{+}{\cdot}Mg^{2+}{\cdot}SO_4^{2-}{\cdot}Cl^{-}$; *3* TDS is between 3,500 and 10,000 mg L^{-1} and the water type is $Na^{+}{\cdot}Cl^{-}$ type; *4* Cities and towns

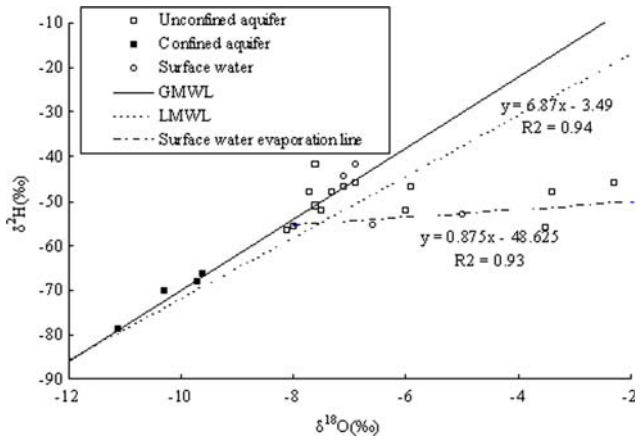

Fig. 5 Plot of $\delta^{18}O$ and $\delta^{2}H$ for groundwater from the Quaternary aquifer system of the Ejina Basin with plots of the GMWL, LWML and surface water evaporation line

GMWL (Fig. 5). This indicates that the groundwater recharge resource mainly source from precipitation, and is weakly affected by evaporation. Second, some isotope compositions of the unconfined aquifer groundwater samples deviate from the GMWL and LMWL, and fall on the surface water evaporation line (Fig. 5). These samples belong to the unconfined aquifer groundwater far away from the riverside. Third, the isotope compositions of the deep confined groundwater samples are close to the

GMWL (Fig. 5) and the influence by evaporation is little. Lastly the deep confined groundwater is notably depleted in heavy isotopes in comparison with unconfined groundwater (Fig. 5). These more depleted signatures are considered to be from the late Pleistocene and Holocene periods, during which the climate was wetter and colder than present day (Zhu et al. 2007).

The tritium content in unconfined aquifer groundwaters ranged from 23 to 49 TU (Table 1). The relative high tritium content (32–49 TU) was located near the river attributed to admixture of surface water with high tritium content. In contrast, the tritium content of the deep confined groundwater was generally less than 1 TU.

Radiocarbon analyses for four deep confined aquifer groundwaters are shown in Table 1 as percent modern carbon (pmc) where the range is from 18.3 to 27.4 pmc. The δ^{13} C values lie between −5.7 and −3.9‰ and have an average value of −4.95‰.

Discussion

Geochemical evolution

The variation of ion concentration in groundwater illustrated that the extent of groundwater–surface water interaction governed groundwater quality in the Ejina Basin. The groundwater samples were collected near the river bank, allowing groundwater to easily be recharged from the river, and assuring a high quality of groundwater. Comparatively, those collected farther from the river, the TDS and concentrations of the major ions generally rose along the flow path of the groundwater, in part because of its greater residence time in the rock formations bearing it and the absence of the influence of surface water recharge.

Dissolved species and their relations with each other can reveal the origin of solutes and the processes that generated the observed composition of water (Hussein 2004). Statistical analyses indicate a positive correlation between some pairs of parameters shown in Fig. 6.

The Na−Cl relationship has often been used to identify the mechanism for acquiring salinity and saline intrusions in semi-arid/arid regions (Sami 1992). The Na^+ and Cl^- show a good correlation (Fig. 6a) indicating that Cl^- and, for the most part, Na^+ are derived from the dissolution of disseminated halite in fine-grained sediments. A principle feature of the groundwater is the enrichment in Na^+ relative to Cl^-, giving molar ratios up to 4.3 (sample no. 10), although the higher salinities of the groundwater mask the effect, to give slightly lower values (Fig. 6b). The high Na/Cl ratios are probably controlled by water–rock interaction, most likely by feldspar weathering via a reaction such as

$$2NaAlSi_3O_8 + 9H_2O + 2H_2CO_3 = Ai_2Si_2O_5(OH)_4 + 2Na^+ + 2HCO_3^- + 4H_4SiO_4. \quad (1)$$

Reaction (1) also produces kaolinite, which is common in weathered rocks of the Ejina Basin. It is revealed by drilling cores that the majority of the feldspars in the middle and lower Pleistocene series rocks in the study area were altered to white kaolinite. A good relationship between Na^+ and SO_4^{2-} (Fig. 6c) suggests another potential source of excess Na^+ is weathering of Glauber's salt (Na_2SO_4). Sediment core from a borehole at the terminal lakes region found the existence of Glauber's salt. The lower Na/Cl ratio of the saline groundwater probably results from ion exchange of Na^+ for Ca^{2+} and Mg^{2+} in clay (discussed below).

In the study area, Ca^{2+}, Mg^{2+}, HCO_3^-, and SO_4^{2-} are mainly derived from the dissolution of crystalline dolomitic limestones and calcium–magnesium silicates, chiefly from calcite, plagioclase, gypsum and feldspar. Although Ca^{2+} and SO_4^{2-} show a good correlation with one another (Fig. 6d), suggesting that simple gypsum dissolution may exert a control on the Ca^{2+} chemistry, there is too little Ca^{2+} relative to SO_4^{2-} for gypsum alone to be responsible for Ca^{2+} chemistry (Fig. 6d). The good correlations between Ca^{2+} and HCO_3^- and between (Ca^{2+} + Mg^{2+}) and HCO_3^- (Fig. 6e, f) suggest that calcite and dolomite weathering also contribute ions to the groundwater. If Ca^{2+}, Mg^{2+}, SO_4^{2-} and HCO_3^- were derived from simple dissolution of calcite, dolomite, and gypsum, then a charge balance should exist between the cations and anions. Specifically, a 1:1 stoichiometry of (Ca^{2+} + Mg^{2+}) to (SO_4^{2-} + HCO_3^-) should exist. However, a deficiency in (Ca^{2+} + Mg^{2+}) relative to (SO_4^{2-} + HCO_3^-) exists in groundwater samples (Fig. 6g), and excess negative charge of SO_4^{2-} and HCO_3^- must be balanced by Na^+, the only other major cation. The main source of Mg^{2+} in groundwater is dolomite in sedimentary rock, which is common in the Ejina Basin. More than 579.6 mg/l (sample no. 12) was observed in the desert zone, where groundwater is saline, and the Mg^{2+}/Ca^{2+} ratios is close or exceeding 1 (Fig. 6h). The high Mg^{2+}/Ca^{2+} ratio (Fig. 6h) strongly indicates that weathering of dolomite or carbonates containing high concentration of Mg^{2+}, which is common in the sedimentary rock, may be important in the Heihe River Basin.

Molar Na/Ca ratios vary between 0.95 (sample no. 21) and 13.5 (sample no. 18), and most of them are of more than 2 (Fig. 6i). This indicated the reaction of silicate minerals and or some cation exchange is occurring at the expense of some cation (Wen et al. 2005; Zhu et al. 2007). This is confirmed by two indices of base exchange (IBE), namely the chloro alkaline indices (CAI 1 and CAI 2) (Schoeller 1965), where

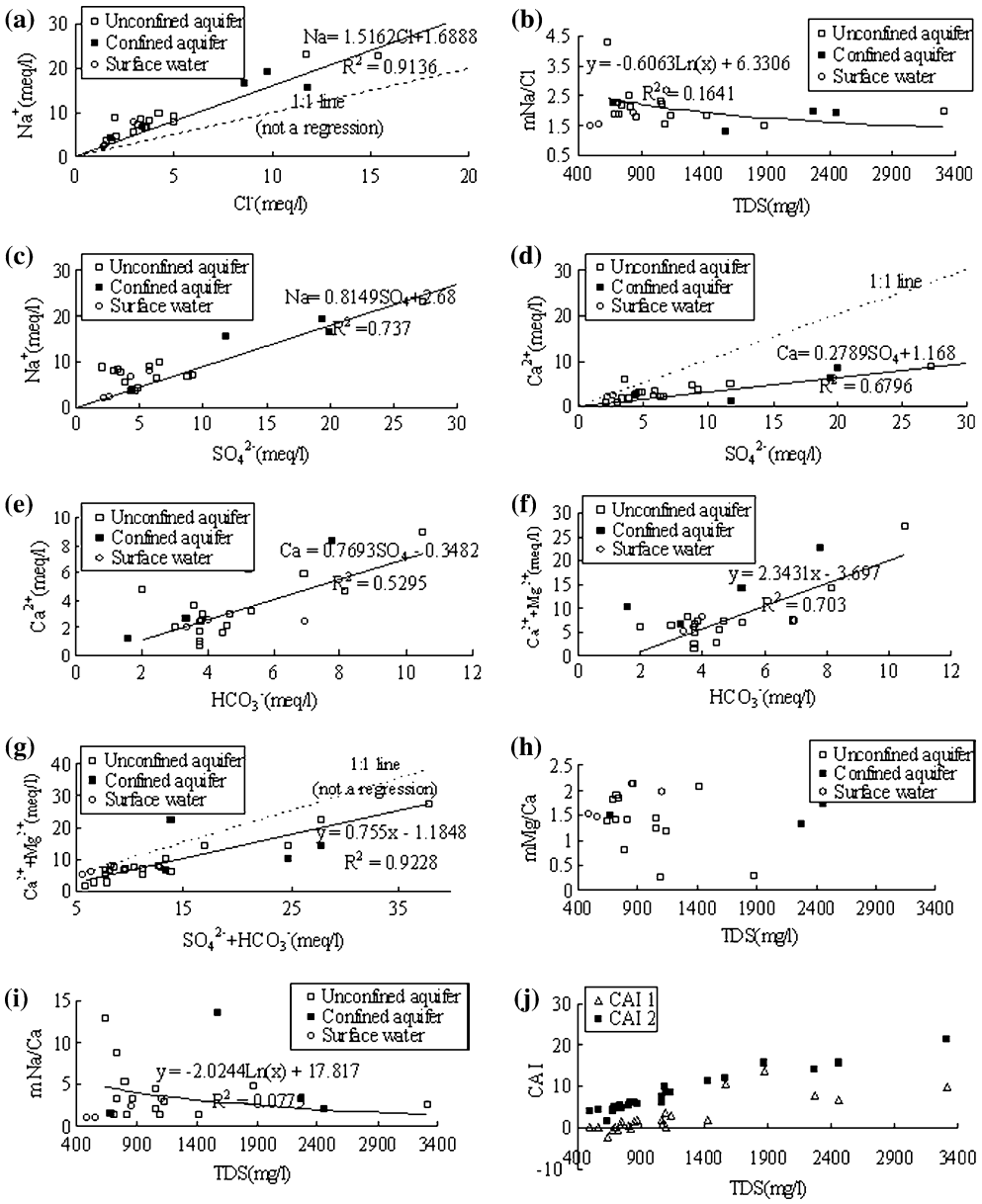

Fig. 6 Major ion relationship: **a** Cl versus Na, **b** Na/Cl versus TDS, **c** SO_4 versus Na, **d** SO_4 versus Ca, **e** HCO_3 versus Ca, **f** HCO_3 versus (Ca + Mg), **g** (HCO_3 + SO_4) versus (Ca + Mg), **h** Mg/Ca versus TDS, **i** Na/Ca versus TDS, and **j** chloro alkaline index (CAI) versus TDS, for groundwater in the study area

$$\begin{cases} \text{CAI} \quad 1 = \text{Cl} - \dfrac{\text{Na+K}}{\text{Cl}} \\ \text{CAI} \quad 2 = \text{Cl} - \dfrac{\text{Na+K}}{\text{SO}_4} + \text{HCO}_3 + \text{CO}_3 + \text{NO}_3 \end{cases} . \qquad (2)$$

When there is an exchange between Na^+ and K^+ in groundwater with Mg^{2+} or Ca^{2+} in the aquifer material, both of the indices are positive, indicating ion exchange of Na^+ in groundwater with Ca^{2+} or Mg^{2+} in the alluvium or weathered materials. In general, these indices show positive values, whereas the low-salt waters give negative CAI 1 values (Fig. 6j). The increase in groundwater salinity was accompanied by a slow rise in reverse ionic exchange, which indicates a cationic exchange that increases the hardness of these waters. The contribution of K^+ to the groundwater in these samples is modest. The low levels of potassium in natural waters are a consequence of its tendency to be fixed by clay minerals and to participate in the formation of secondary minerals.

As illustrated in the Gibbs plot in Fig. 7 (Gibbs 1971, 1970), other dominant processes determining the water composition are evaporation and precipitation. Evaporation of surface water and moisture in the unsaturated zone has been found as the most influential process in the development of the chemical composition of shallow

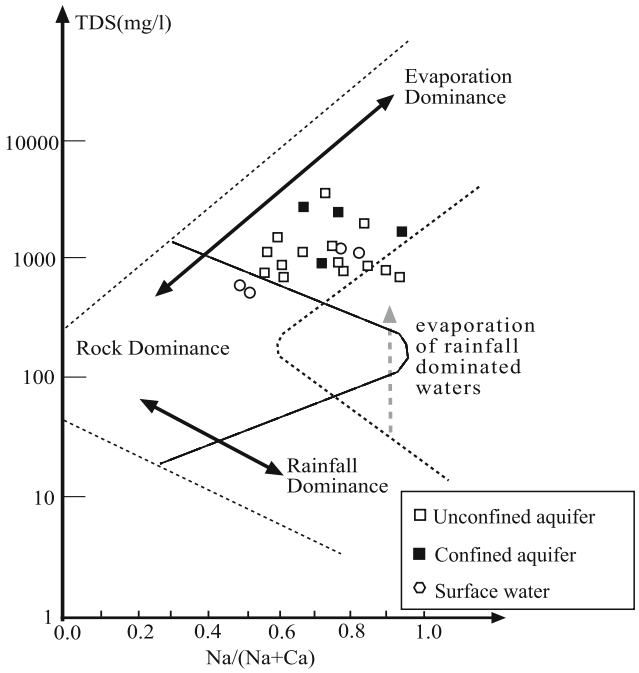

Fig. 7 A Gibbs plot indicating the mechanisms that determine the major ion composition of groundwater in Ejina Basin

groundwater (Richter and Kreitler 1993). Evaporation concentrates the remaining water and leads to precipitation and deposition of evaporates that are eventually leached into the saturated zone. This source of groundwater salinity is amplified in arid lands, such as the study site, due to the high evaporation rate and low rainfall which encourage the above-mentioned processes and also lower flushing of saline water. This is clearly reflected in the Gibbs plot, which indicates a trend towards evaporation (and precipitation of the least soluble minerals) in the terminal lake region, and rock-dominated weathering within the river water influence zone. Mineral equilibrium calculations for groundwater are useful in predicting the presence of reactive minerals in the groundwater system and estimating mineral reactivity (Deutsch 1997). By using the saturation index (SI) approach, it is possible to predict the reactive mineralogy of the subsurface from groundwater data without collecting the samples of the solid phase and analyzing the mineralogy (Deutsch 1997). In the present study, to determine the chemical equilibrium between minerals and water, SI of calcite, dolomite, and gypsum were calculated based on the following equation (Lloyd and Heathcote 1985):

$$\mathrm{SI} = \log\left(\frac{\mathrm{IAP}}{K_S(T)}\right) \tag{3}$$

where IAP is the ion activity product of the solution, and K_S (T) is the equilibrium constant of the reaction considered at the temperature T.

The calculated values of SI for calcite, dolomite and gypsum range from −1.03 to 0.84, −1.18 to 1.98, and −2.28 to −0.52 with averages 0.04, 0.31, and −1.53, respectively. About 60% of the groundwater samples were kinetically oversaturated with respect to calcite and dolomite, and all the samples were below the equilibrium state with gypsum.

Mean residence time of the shallow groundwater

Tritium ^{3}H, with its half-year 12.32 years (Lucas and Unterweger 2000) has been widely used for the estimation of recent groundwater residence time. The reason for this is because tritium constitutes part of the water molecule, and thus its behavior is identical to that of groundwater. Once ^{3}H enters the subsurface as meteoric water, it becomes isolated from the influences of variable atmospheric ^{3}H concentrations. Concentrations of ^{3}H in the groundwater system depend primarily on the initial atmospheric concentration at the time of recharge and the radiogenic decay that has occurred since infiltration. In some cases, investigators have interpreted approximate groundwater ages from ^{3}H concentrations. Several models have been suggested as appropriate for use of tritium in the estimation of mean residence time of groundwater (Maloszewski and Zuber 1996).In this study, the exponential distribution function (Fontes 1983; Yurtsever 1983), coupled with the hypothesis of a completely mixed reservoir, was applied. The required tritium input function for this simulation was taken from the available tritium records of Zhangye station, which is the closest IAEA network station to the study area. The IAEA's network of pluviometer in Zhangye can provide the monthly precipitation tritium concentration from 1983. In order to infer what the historic distribution of tritium has been in precipitation in the region, it is necessary to reconstruct the earlier missing tritium values for Zhangye station during the period 1953–1982. Thus, the tritium values in precipitation during 1953–1959 were approximated from the correction with the data of Ottawa, Canada, which has the longest tritium content records globally; while the values during the period of 1960–1986 were estimated from the Doney model (Doney et al. 1992). The tritium input function of Zhangye station is shown in Fig. 8. Tritium concentration in precipitation reached its maximal value of 4,637.2 TU in 1964. Since that time, the amount of tritium in precipitation has decreased almost exponentially. At present day, the tritium content in precipitation basically maintains around 40 TU (Fig. 8).

The simulated tritium output curves were calculated using the convolution integral expressed by:

$$C_{\text{out}}(t) = \int_0^{\infty} C_{\text{in}}(t-\tau)\mathrm{e}^{-\lambda\tau} g(\tau)\mathrm{d}\tau \quad (4)$$

where

$$g(\tau) = \frac{1}{\tau_0}\mathrm{e}^{-(1/\tau_0)\tau} \quad (5)$$

and

$$\tau_0 = \frac{V}{Q} \quad (6)$$

where λ is the radioactive decay, τ_0 is the mean residence time (MRT) of the system, and V and Q are the volume of groundwater reservoir and the discharge of the system, respectively.

The calculation of tritium output curves for different values of MRT for 5, 25, 60, 120, 500, 2,000, 3,000 years are shown in Fig. 9. According to the simulated output curves, the tritium content during the period 2000–2004 should be of the order of 50 TU, if the residence time was about 5 years. In parallel, if the residence time of the groundwater was 120 years, then the observed tritium value in the groundwater was about 20 TU. But if the residence time of the groundwater exceeds 500 years, the observed tritium value should less than 10 TU, and if the tritium content was less than 1 TU, this model reveals that the residence time exceeds 3,000 years. This result was also proven throughout the radiocarbon groundwater age calculation, and is discussed further. Comparison of the calculated output curves with the observed tritium values suggests a mean turnover time between 5 and 120 years. Thus, the unconfined groundwater is renewable, but it is highly dependent on the Heihe River water. In order to maintain and recovery the fragile ecological environmental in the Ejina Basin, a considerable discharge of the Heihe River must be assured, and co-operation between the upper, middle and lower reaches of the Heihe River is needed in the exploitation, use, management and protection of water resources.

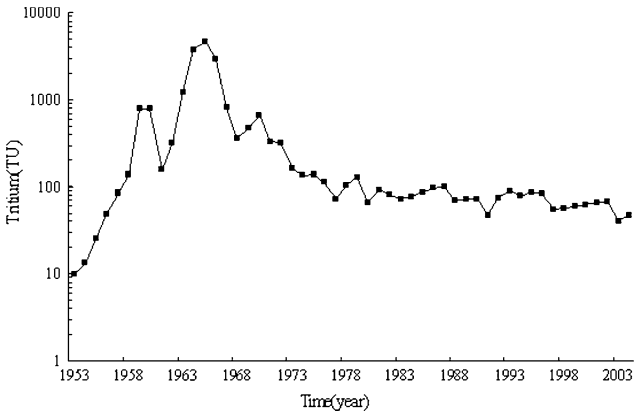

Fig. 8 The reconstructed tritium values from 1953 to 1982 in Zhangye station with a plot of observation data from 1983

In contrast, the tritium content of the deep confined groundwater was generally less than 1 TU. This suggested more than 3,000 years residence time may be existed in the confined groundwaters, and a radiocarbon groundwater age calculation was needed (see below).

Deep groundwater age dating

Groundwaters in the confined aquifer with relatively low tritium content were supposed to be recharged before 1952. Their ages were determined by ^{14}C dating methods. Generally, based on the fundamental law of radioactive decay, it is possible to calculate the groundwater age (t) by

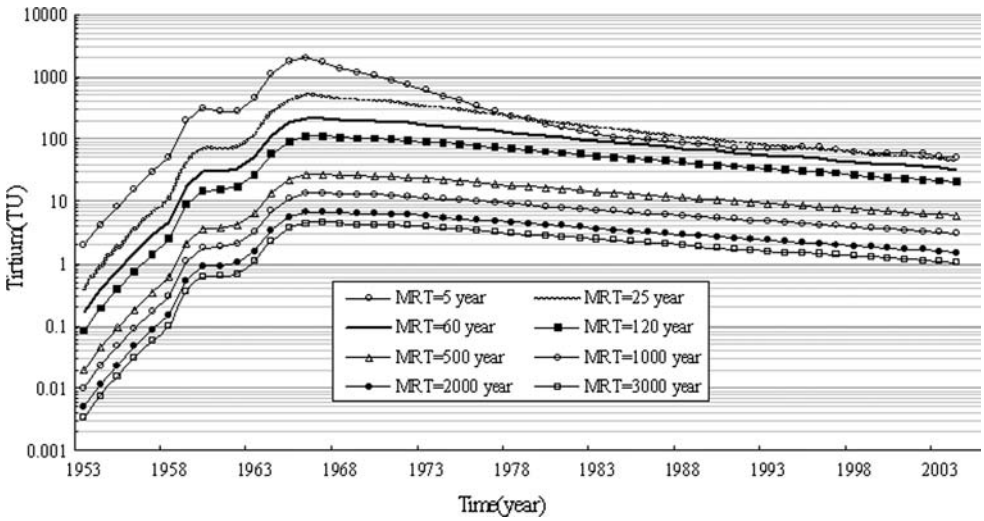

Fig. 9 Calculated tritium output curves for different mean residence time (MRT)

measuring its ^{14}C activity (A_t) and by knowing the initial ^{14}C activity (A_0), in the following formula:

$$t = \frac{\tau}{\log 2} \log \frac{A_0}{A_t} \quad (7)$$

where τ is the half-life of ^{14}C ($\tau = 5,730 \pm 30a$).

Although the formula is simple, the estimation of the initial ^{14}C activity (A_0) is still a difficult task in isotope hydrology. There were several correction models to estimate the initial ^{14}C activity (Vogel 1970; Tamers 1975; Pearson 1965; Mook 1976; Fontes and Garnier 1979). The corrected groundwater ages according to the different correction models are complied in Table 2. The uncorrected ages are significantly higher than those calculated by other different models. The groundwater ages calculated according to Vogel concept are also high compared with the other corrected ones, but less than about 1,846 years as compared with the uncorrected ages. The Tamers, Pearson, and Fontes and Garnier models gave a similar mean initial ^{14}C activity (A_0), 51.8 ± 1.2, 51.2 ± 1.2, and 48.6 ± 12.6, respectively. However, the Eichinger and Gonfiantini model gave a low mean A_0 (31.0 ± 3.4 pmc). The groundwater ages calculated by the Tamers model were similar to those calculated according to the Pearson model (Table 2) with a maximum difference of 1,213.9 years, and likely to be the most representative. Both the Tamers model ages and the Pearson model ages were not far from ages calculated with the Fontes and Garnier model, while the Eichinger and Gonfiantini model actually overcorrected the ages.

In view of Tamers model and Pearson model ages, the deep confined groundwater falls in an age bracket of 4,087–9,364 years BP. Stable isotopes ($\delta^{18}O$ and $\delta^{2}H$) provide clear distinction between modern and ancient waters. Deep confined groundwater samples have depleted levels of isotope content compared with those collected from unconfined wells (Fig. 5). Thus, it is almost certain that deep confined groundwater in the Quaternary aquifer was recharged during a period in the past when the climate was wetter and colder. This conclusion is in line with the general observations from the nearby Minqin Basin and Badain Jaran Desert (Ma and Edmunds 2006). Thus, air mass circulation over this region during the late Pleistocene and Holocene was significantly different from the present day, with evidence of a strengthened monsoon during this period. Chen et al. (2003) also observed in the North China Plain near Beijing a progressive enrichment in $\delta^{18}O$ values from about 7 ka BP and an optimum around 6–4 ka BP equivalent to the global warming and a strengthened monsoon.

The results also indicate that the ages increased towards the north and west in the Ejina Basin. Samples collected around Ejina city (sample nos. 16 and 18) and Saihantaolai city (sample nos. 17 and 19) have ages ranging from 5,300 to 8,695 years (Table 2). The ^{14}C ages from sample nos. 17 and 19 can be used to determine the approximate groundwater flow velocity. The older sample (8,695 years) is ~20 km further down gradient than the younger (6,929 years). This yields an approximate flow velocity of 11.3 m/year. Using Darcy's Law, the estimated groundwater velocity between sample nos. 20 and 21, assuming an average porosity of 0.11, hydraulic conductivity of 2.4 m/day, and a hydraulic gradient of 1.5×10^{-3} (Wu 1999), is 11.9 m/year. The result is basically consistent with that calculated by ^{14}C dating, and indicates that groundwater flow of the deep confined aquifer is relatively slow and the water resources are non-renewable.

The scientific results have important implications for groundwater management in the Heihe River Basin, probably the most water-stressed of the basins in northwest China and in a region destined for rapid development under China's West Development Strategy. Since the bulk of the deep confined water resource was derived from recharge during a past wetter climate and its present day recharge is limited, and if more water is withdrawn than is replenished, exploitation of this groundwater is considered to be 'mining' (Chen et al. 2004). In particular, the basin has seen over-exploitation of water resources due to a lack of rational planning and effective water saving measures. Groundwater recharge is decreasing, water levels are falling, and water quality is getting worse (Qi and Luo 2005). To curb such 'eco-hydrological deterioration', one should minimize water wastage by developing and encouraging the use of more efficient irrigation techniques, increase the rate of water reuse in agriculture, industries and settlements, and set up a rational land-use plan for agriculture,

Table 2 Groundwater ages determined by application of the most commonly used models in isotope hydrology

Site no	Uncorrected age (year BP)	Vogel age (year BP)	Tamers age (year BP)	Pearson age (year BP)	Fontes and Garnier age (year BP)	Eichinger and Gonfiantini age (year BP)
16	11,022.0	9,175.3	5,301.6	4,087.7	1,702.7	−65.7
17	12,381.8	10,535.1	6,929.7	7,046.3	6,421.5	2,892.9
18	10,928.5	9,081.8	5,643.6	5,593.0	7,119.1	1,439.6
19	14,054.9	12,208.1	8,695.3	9,364.6	8,323.2	5,211.2

forestry, and animal husbandry to regulate water allocation on a whole-basin basis. This will help to ensure continued socio-economic development and the protection of the fragile ecology.

Conclusions

The hydrochemical and isotope investigation was conducted in the Ejina Basin to understand the geochemical evolution and the residence time of the groundwater. The main conclusions are as follows:

The trends in major elements in the Ejina Basin groundwaters show a progressive sequence of geochemical evolution. Overall the groundwater in the recharge area is of $Na^+ \cdot HCO_3^-$ type with low TDS, less than 1,000 mg/l, changing to $Na^+ \cdot Mg^{2+} \cdot SO_4^{2-} \cdot Cl^{-1}$ or $Na^+ \cdot Mg^{2+} \cdot Cl^{-1} \cdot SO_4^{2-}$ type with TDS, 1,000–3,800 mg/l along the groundwater flow direction and finally becoming to $Na^+ \cdot Cl^{-1}$ with TDS higher than 5,000 mg/l. From the ion-ratio plot, the rock weathering and evaporation are dominant factors that determine the major ionic composition in the study area. In addition to the dissolution of halite, the high ratio of $(Na^+ + K^+)/Cl^-$ indicates a significant contribution of dissolved ions from silicates weathering. Another potential source of excess Na^+ is weathering of Glauber's salt (Na_2SO_4). Gypsum in anhydrite dissolution is mainly responsible for Ca^{2+} and SO_4^{2-}. Other chemical processes adding calcium is cation exchange. The high Mg^{2+}/Ca^{2+} ratio indicates that weathering of Mg-rich dolomite, which is common in the sedimentary rock in Heihe River Basin, may be involved. The SI of calcite, dolomite is generally greater than zero, which suggests that these minerals are deposited.

Most stable isotopes composition of $\delta^{18}O$ and $\delta^{2}H$ of groundwater in the Ejian Basin is meteoric water features. The deep confined groundwater is markedly deleted in heavy isotopes comparing with unconfined groundwater. Enrichment of stable isotopes by evaporative in desert region implies an evaporative process occurring at or near the soil surface above the zero flux plane before deep percolation.

Based on tritium content in the atmospheric precipitation and by adopting a model with exponential time distribution function, the mean residence time of the shallow groundwater of Ejian Basin is 5–120 years. The shallow groundwater mainly gets its supply from the river. So, a considerable discharge of the Heihe River must be assured to maintain and recovery the fragile ecological environmental in the Ejina Basin. The ^{14}C deep confined groundwater ages ranging between 4,087 and 9,364 years BP are in good agreement with the paleo-climatic humid and cold conditions that prevailed during the late Pleistocene and the early Holocene.

Acknowledgments This research was supported by a grant from the National Natural Science Foundation of China (Nos. 40701054 and 40671010), and National Social Science Foundation of China (No. 08XJY009). Special thanks to Dr. T. Martin-Crespo and another anonymous reviewer for their critical reviews and helpful comments.

References

Chen LH (1996) Desertization and its control in the lower reach of the Heihe River. J Nat Resour 2:35–42 (in Chinese)

Chen Z, Qi J, Xu J, Ye H (2003) Palaeoclimatic interpretation of the past 30 kyr from isotopic studies of the deep confined aquifer of the North China Plain. Appl Geochem 18:997–1009

Chen ZY, Nie ZL, Zhang GH, Wan L, Chen XX, He ML (2004) Groundwater renewability based on groundwater ages in the Heihe valley alluvial Basin, Northwestern China. Acta Geol Sin 4:560–567 (in Chinese)

Craig H (1961) Isotopic variations in meteoric waters. Science 133:1702–1708

Dansgarrd W (1964) Stable isotopes in precipitation. Tellus 16(4): 436–468

Deutsch WJ (1997) Groundwater geochemistry: fundamentals and application to contamination. CRC Press, Boca Raton

Doney SC, Glover DM, Jenkins WJ (1992) A model function of the global bomb tritium distribution in precipitation, 1960–1986. J Geophys Res 97:5481–5492

Eichinger L (1980) Experience gathered in low-level measurement of ^3H in water. In: Low-level ^3H measurement, IAEA, Vienna, pp. 43–64 (TECDOC–246)

Esteller MV, Andreu JM (2004) Anthropic effects on hydrochemical characteristics of the Valle de Toluca aquifer (central Mexico). Hydrogeol J 13:378–390

Fan XP (1991) Characteristics of the stream-aquifer systems and rational utilization of water resources in the Heihe River. Gansu Geol 12:1–16 (in Chinese)

Feng Q, Wei L, Su YH, Zhang YW, Si JH (2004) Distribution and evolution of water chemistry in Heihe River Basin. Environ Geol 45:947–956

Fontes JC (1983) Dating of groundwater. In: Guidebook on nuclear techniques in hydrology (Technical Report, Series no 91), IAEA, Vienna

Fontes JC, Garnier JM (1979) Determination of the initial ^{14}C activity of the total dissolved carbon: a review of the existing models and a new approach. Water Resour Res 15:399–413

Fritz P, Fontes JC (1980) Handbook of environmental isotope geochemistry. Elsevier, Amsterdam

Gao Q, Li F (1990) Rational development and utilization of water resources in the Heihe River basin of Northwest China. Gansu Press of Science and technology, Lanzhou, pp 23–95 (in Chinese)

Gao Q, Wu Y, Liu F (2004) Unified management of water resources and enhance of carrying capacity in Heihe River Basin. J Desert Res 24(2):156–161 (in Chinese)

Gibbs R (1970) Mechanism controlling world river water chemistry. Science 170:1088–1090

Gibbs R (1971) Mechanism controlling world river water chemistry: evaporation-crystallization process. Science 172:871–872

Harrison TM, Copeland P, Kidd WSF, An Y (1992) Raising Tibet. Science 255:1663–1670

Hussein MT (2004) Hydrochemical evaluation of groundwater in the Blue Nile Basin, eastern Sudan, using conventional and multivariate techniques. Hydrogeol J 12:144–158

IAEA (1980) Arid zone hydrology: investigations with isotope techniques. In: Proceeding of an advisory group meeting, International Atomic Energy Agency, Vienna, 265 pp

IAEA (1983) Palaeoclimates and palaeowaters: a collection of environmental isotope studies. In Proceedings of an advisory group meeting, International Atomic Energy Agency, Vienna, 207 pp

Ji XB, Kang ES, Zhao WZ, Cheng RS, Xiao SC, Jin BW (2005) Analysis on supply and demand of water resources and evaluation of the security of water resources in irrigation region of the middle reaches of Heihe River, Northwest China. Sci Agric Sin 38(5):974–982 (in Chinese)

Li JJ, Wen S, Zhang Q (1979) Study on the times, extent and form on Tibet plateau upheaving. Sci China 9:608–616

Lloyd JW, Heathcote JA (1985) Natural inorganic hydrochemistry in relation to groundwater. Oxford University Press, New York

Lucas LL, Unterweger MP (2000) Comprehensive review and critical evolution of the half-life of tritium. J Res Natl Inst Stand Techno 105(4):541–549

Ma JZ, Edmunds WM (2006) Groundwater and lake evolution in the Badain Jaran Desert ecosystem, Inner Mongolia. Hydrogeol J 14:1231–1243

Ma JZ, Wang XS, Edmunds WM (2005) The characteristics of groundwater resources and their changes under the impacts of human activity in the arid Northwest China—a case study of the Shiyang River Basin. J Arid Environ 61:277–295

Maloszewski P, Zuber A (1996) Lumped parameter models for the interpretation of environmental tracer data. In: Manual on mathematical models in isotope hydrology. IAEA, Vienna, pp. 9–58

Molner P, Tapponnier P (1975) Cenozoic tectonic of Asia: effects of a continental collision. Science 189:419–426

Mook WG (1976) The dissolution-exchange model for dating ground water with carbon-14. In: Interpretation of environmental isotope and hydrochemical data in ground water hydrology. IAEA, Vienna, pp. 213–225

Narasimhan TN (2005) Hydrogeology in North America: past and future. Hydrogeol J 13:7–24

Pearson FJ (1965) Use of C-13/C-12 ratios to correct radiocarbon ages of material initially diluted by limestone. In: Proceedings of the 6th International Conference on Radiocarbon and Tritium Dating, Pulman, WA, pp. 357–366

Qi SZ, Luo F (2005) Water environmental degradation of the Heihe River Basin in arid Northwestern China. Environ Monit Assess 108:205–215

Richter BC, Kreitler WC (1993) Geochemical techniques for identifying sources of groundwater salinization. CRC Press, New York

Sami K (1992) Recharge mechanisms and geochemical process in a semi-arid sedimentary basin, Eastern cape, South African. J Hydrol 139:27–48

Schoeller H (1965) Hydrodynamique dans le karst (Hydrodynamics of karst). Actes du Colloques de Doubronik. IAHS/UNESCO, Wallingford, pp 3–20

Shi JA, Wang Q, Chen GJ, Zhang ZN (2001) Isotopic geochemistry of the groundwater system in arid and semiarid areas and its significance: a case study in Shiyang River Basin, Gansu Province, northwest China. Environ Geol 40:557–565

Shi Y, Zhang X (1995) The influence of climate changes on the water resources in arid areas of northwest China. Sci China B 25:968–977

Tamers MA (1975) Validity of radiocarbon dates on groundwater. Geophys Surv 2:217–239

Vogel JC (1970) Carbon-14 dating of groundwater. In: Proceedings of a symposium on isotope hydrology, IAEA, Vienna, pp. 225–239

Wen X, Wu Y, Zhang Y, Liu F (2005) Hydrochemical characteristics and salinity of groundwater in the Ejina basin, Northwestern China. Environ Geol 48:665–675

Wu X (1999) The status of hydrogeological research in arid and semiarid zone. J Hydrogeol Eng Geol 4:41–46 (in Chinese)

Wu Y, Wen X, Zhang Y (2004) Analysis of the exchange of groundwater and river water by using Radon-222 in the middle Heihe Basin of Northwestern China. Environ Geol 45:647–653

Xiao HL (2000) Resource environment and management of water resource in China. Kaiming Press, Beijing (in Chinese)

Yurtsever Y (1983) Models for tracer data analysis. In: Guidebook on nuclear techniques in hydrology. Technical Report, Series no 91. IAEA, Vienna

Zhang YH, Wu Y, Su J, Wen X, Liu F (2005) Groundwater replenishment analysis by using natural isotopes in Ejina Basin, northwestern China. Environ Geol 48:6–14

Zhu GF, Li ZZ, Su YH, Ma JZ, Zhang YY (2007) Hydrogeochemical and isotope evidence of groundwater evolution and recharge in Minqin Basin, Northwest China. J Hydrol 333:239–251

Zhu YH, Wu YQ, Sam D (2004) A survey: obstacles and strategies for the development of ground-water resources in arid inland river basins of Western China. J Arid Environ 9:351–367

Zuhair K (2001) Use of hydrochemistry and environmental isotopes for evaluation of groundwater in the Paleogene limestone aquifer of the Ras Al-Ain area (Syrian Jezireh). Environ Geol 41:128–144